Received 26 November 2022; revised 5 January 2023; accepted 19 January 2023. Date of publication 23 January 2023; date of current version 21 February 2023.
The review of this article was arranged by Editor K. Joshi.

Digital Object Identifier 10.1109/JEDS.2023.3239100

RF Overdrive Burnout Behavior and Mechanism Analysis of GaN HEMTs Based on High Speed Camera

CHANG LIU[1], HONG XIA LIU[1], YI QIANG CHEN[2] (Member, IEEE), YI JUN SHI[2], YU HAN XIE[2], SI CHEN[2], PING LAI[2] (Member, IEEE), ZHI YUAN HE[2], AND YUN HUANG[2]

1 School of Microelectronics, Xidian University, Xi'an 710071, Shannxi, China
2 Fifth Electronics Research Institute, Ministry of Industry and Information Technology, Guangzhou 511370, Guandong, China

CORRESPONDING AUTHORS: C. LIU, H. X. LIU, AND Y. Q. CHEN (e-mail: xd_liuchang@163.com; hxliu@mail.xidian.edu.cn; yiqiang-chen@hotmail.com)

This work was supported in part by the National Natural Science Foundation of China under Grant U2241221, Grant 52107184, and Grant 62274043; and in part by the Guangzhou Basic and Applied Basic Research Project under Grant 202201010868.

ABSTRACT In this work, a new method for failure analysis of electronic components, high speed camera, is used to investigate burnout failure location of GaN HEMTs under RF overdrive stress. Based on the high speed camera system and the RF test system, we can filter out most of the burn flashes, and clearly locate the weak parts of devices. To further explain the burnout mechanism, a long-term (100 h) RF overdrive stress experiment was carried out and the significant degradation was observed. The drain-source current decreases and the threshold voltage drifts forward. These phenomena show that the degradation of RF overdrive stress is based on hot electron effect (HEE), which is related to the electric field. Besides, Electroluminescence (EL) tests are used and the non-uniform but strong luminescence characteristics of the gate were found, which indicates the strong electric field is the main cause of burnout. We also explore the correlation between burnout and ambient temperature. It was found that the influence of ambient temperature on the burnout was limited. At last, a TCAD simulation is carried out to confirm the temperature and electric field distribution in the device when burnout. It can be found that the electric field inside the device exceeded the breakdown electric field of GaN, which further proves that the burnout caused by RF overdrive is mainly due to electric field rather than temperature.

INDEX TERMS GaN HEMTs, burnout, RF overdrive stress.

I. INTRODUCTION

Among all the reliability problems, burnout is far and away the most destructive. The burnout of electronic components will result in the loss of all device functions and the whole system collapse. Due to the excellent characteristics of GaN HEMTs, they are often used in high power fields [1], [2], leading to a frequent occurrence of burnout failure. In particular, RF overdrive stress is one of the important reasons for GaN HEMTs' burnout [3]. RF overdrive stress refers to the stress when the input power exceeds maximum rated input power of devices. This phenomenon often occurs in practical applications. Especially in phased array radar with a large number of T/R components, in which GaN HEMTs play the role of the last stage power amplifier. In order to ensure a high output power, most of the components tend to work in saturation state, but due to the differences between components, some components may be under the influence of RF overdrive stress, thus affecting the reliability of the components [4], [5], [6], [7]. In addition, high power microwave based on electronic warfare can also cause devices to be in RF overdrive state [8], [9]. When the RF overdrive stress is too high, the device will be burnt out. However, in previous studies, burnout is often lack of systematic research. This is mainly based on two reasons: 1) The phenomenon of burnout failure is often instantaneous and lasts in the order of microsecond, which is difficult to be detected by common observation equipment; 2) The device structure after burnout is completely destroyed, so it is difficult to analyze the initial

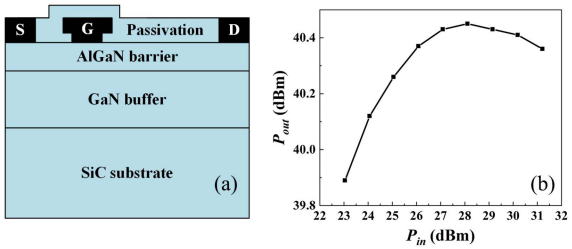

FIGURE 1. (a) The schematic diagram and (b) output power characteristics of the AlGaN/GaN HEMT near saturation power.

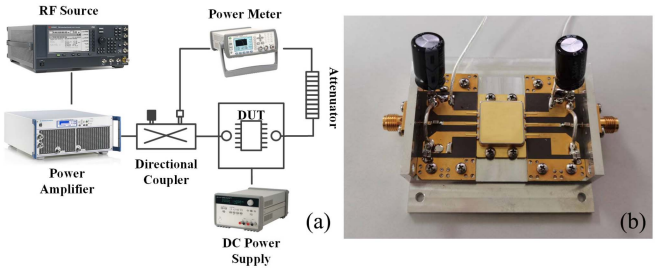

FIGURE 2. (a) RF test system and (b) RF text fixture.

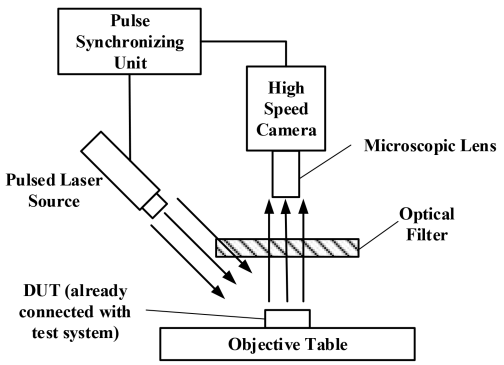

FIGURE 3. High speed camera system.

burned position and carry out failure analysis. Due to these two reasons, device manufacturers cannot accurately locate the weak links in the device, so as to carry out targeted reinforcement design. Therefore, an advanced analytical method is needed to capture and study the burnout process in detail. In this paper, high speed camera is used to study burnout failure and its high frame rate shooting can solve the two problems mentioned above.

There are several researches on GaN devices burnout failure in the earlier stage [10], [11], [12], [13]. But most of the researches uses the simulation method and lacks the monitoring of the burnout process. High speed cameras are also often used in scientific research [14], [15]. But the application of high speed cameras in the field of electronic components is relatively rare because of the small size of the observed sample and the need for strong light source. The system in this paper successfully solves these problem, so as to realize the high speed dynamic capture of the device.

II. EXPERIMENTAL DETAILS

The sample used this paper is commercial GaN HEMT internal matched power amplifier, which operates at 1.146∼1.236 GHz and adopts continuous wave operation mode. The device adopts a SiC substrate with a gate length of 0.35 μm and a gate width of 3.6 mm. The schematic diagram of the structure is shown in Figure 1(a) and the output power characteristics is shown in Fig. 1(b).

In order to apply RF overdrive stress, the RF test system as shown in Fig. 2(a) was built. It includes a RF source, a power amplifier, a directional coupler, an attenuator and a dual channel power meter. The power meter monitors the input and output power of the sample through the coupling end of the coupler and the output end of the attenuator. GaN HEMTs are mounted on a specially designed fixture (Fig. 2(b)) to inject RF power through a coaxial interface.

Burnout experiment and long-term stress experiment were carried out respectively to analyze the failure mechanism of the devices, In the RF overdrive burnout experiment, the input power of the devices was increased continuously to reveal the damage limit value. First of all, the device source-drain voltage (V_{DS}) and the gate-source voltage (V_{GS}) are set as the rated operating voltage. Frequency f is set as a certain frequency point of the operating bandwidth. The input power (P_{in}) is initially set to be 3dB less than the saturation input power. After the experiment began, P_{in} was continuously increased in steps of 1dB and maintained for 1 minute at each input power level. The electrical performance parameters such as output power (P_{out}) and drain-source current (I_{DS}) at each input power are recorded. In order to prevent gate voltage drift under RF overdrive stress, an appropriate resistor (5.5 kΩ) is connected to the gate of the device in series. In this experiment, V_{DS} was maintained at 28V and V_{GS} at -2.5V, $f = 1.15$GHz. While in long-term RF overdrive stress experiment, the input power of the device is set to 10dB above its saturation input power and maintained for 100 hours. V_{DS} was also maintained at 28V and V_{GS} at -2.5V, $f = 1.15$GHz. There is also a 5.5 kΩ resistor is connected to the gate of the device in series. The DC Characteristics of the devices before and after the experiment are measured.

Fig. 3 shows the high speed camera system used in the RF overdrive burnout experiment, including the high speed camera, microscopic lens, optical filter, objective table, pulse laser source and pulse synchronizing unit. The pulse laser source can emit high intensity monochromatic laser, and the optical filter can filter out the light of other wavelengths except the monochromatic laser, so as to prevent the strong light of burnout from affecting the quality of photography. The pulse synchronization unit keeps the frequency of the pulse laser source consistent with the frame number of the high speed camera, which ensures that the brightness of the camera meets the demand. The high speed cameras have the ability to record images automatically, and the last few seconds of images can be preserved by manually stopping

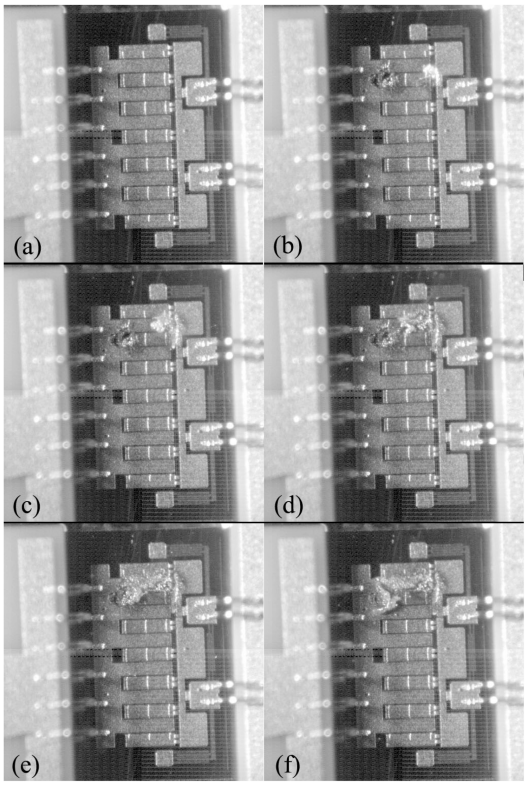

FIGURE 4. A high speed camera photography of the device burnout process. (a) 0 μs, (b) 20 μs, (c) 40 μs, (d) 60 μs, (e) 80 μs, (f) 100 μs.

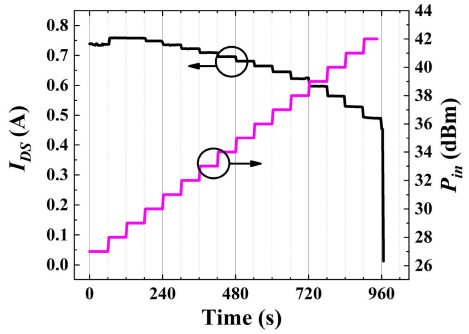

FIGURE 5. The current monitoring results of the device in the burnout process.

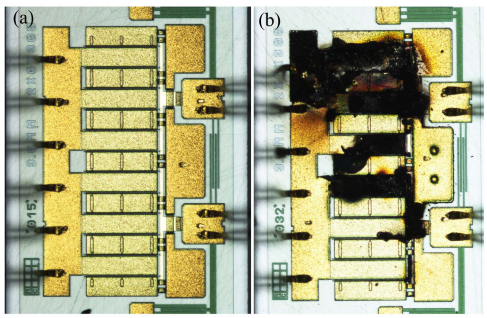

FIGURE 6. A microscope photograph of (a) a fresh device and (b) the burnout device after RF overdrive.

the recording when the device burns out. In this experiment, the camera resolution is set to 512 × 512 and the frame rate is set to 50,000 FPS.

III. RESULTS AND DISCUSSIONS

A. ANALYSIS OF RF OVERDRIVE BURNOUT PROCESS BASED ON HIGH SPEED CAMERA

Fig. 4 shows the whole process of device burnout under RF overdrive stress filmed by high speed camera. Considering the 50,000 FPS frame rate used in this experiment, so the time interval between every two pictures is 20 μs. The 6 images in Fig. 4 show the burnout process in its entirety, so the entire phenomenon of burnout lasted 100 us. By looking closely at the difference between the first and second images, the location of the initial burn point can be found. It was obvious that the second gate from the top was damaged first and the initial burn point is the position between gate and drain. Many studies have shown that the gate edge near the drain of GaN HEMT is where the electric field intensity is greatest, so the burnout position should correspond to the position with the maximum electric field [16], [17], [18]. The damage of the second gate from the top probably means that there is a more concentrated field intensity at the gate.

Fig. 5 shows the current monitoring results of the device in the burnout process. It can be found that, before reaching saturation, I_{DS} increases with the increase of the input power, while in the overdrive state, I_{DS} gradually decreases, because in the overdrive state, the gain of the device decreases, so does the output power. Finally, when the input power reaches 42dBm, the device suddenly burns out.

Microscope photograph of a fresh devices and the burnout device are shown in Fig. 6. It can be seen that the device structure is damaged in a large area after burnout. It is difficult to confirm the initial burn point only by routine microscopic examination.

B. DEGRADATION BEHAVIORS AND MECHANISM ANALYSIS AFTER A LONG-TERM RF OVERDRIVE STRESS

In order to accurately analyze what factors are related to device burnout under RF overdrive stress, a 100h long-term stress experiment is carried out and the electrical characteristics of the device were tested before and after the experiment. Figure 7(a) shows the output characteristics before and after the experiment. The test conditions are V_{GS} ranging from −3.25V to −1.75V at 0.25 V step. As can be seen, the saturation output current of the device is significantly reduced after 100 hours of RF overdrive stress. Comparing the I_{DS} current at $V_{DS} = 5$ V and $V_{GS} = -1.75$ V, it was found that the I_{DS} value decreased from 831mA to 729mA by 12.3%. The transfer and transconductance characteristics before and after the experiment are shown in Fig. 7(b). It can be found that the threshold voltage of the device after the experiment shifts forward from −2.55 V to −2.40 V and the maximum transconductance was also reduced from 724 mS to 661 mS.

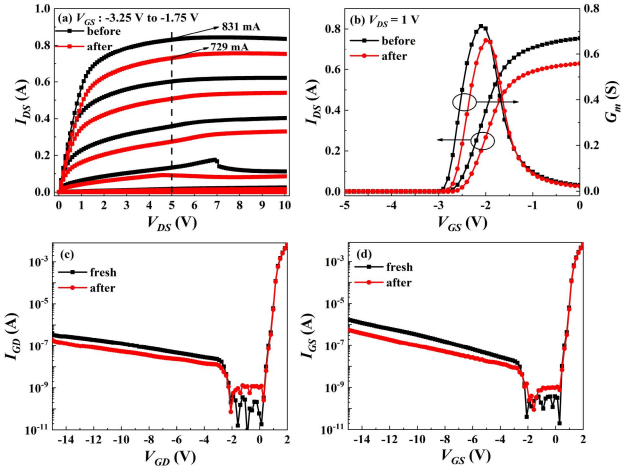

FIGURE 7. DC characteristics of AlGaN/GaN HEMTs before and after long-term RF overdrive stress experiment: (a) output characteristics with V_{GS} ranging from −3.25 to 0 V at 0.25 V step, (b) transfer and transconductance characteristics at V_{DS} = 1 V, (c) gate-to-drain characteristics, and (d) gate-to-source characteristics.

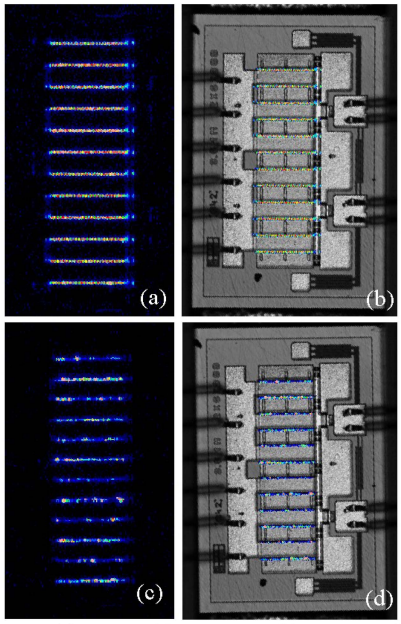

FIGURE 8. (a) EL image with saturated input power, (b) corresponding relationship between luminescent position and device structure with saturated input power 10dB, (d) corresponding relationship between luminescent position and device structure with input power exceeding saturated input power 10dB.

Furthermore, gate-to-drain characteristics and gate-to-source characteristics were also measured before and after the experiment to analyze the effect of long-term RF overdrive stress on the Schottky gate as shown in Fig. 7(c) and (d). As can be seen, the gate leakage current in the negative bias part of the gate decreased slightly. This indicates that the stress does not generate new traps, but rather that the hot electrons fill the traps of the barrier layer or reduce the interface state density [19].

As we seen, the degradation phenomenon of devices after long-term RF overdrive stress is consistent with previous literature [4], [20], [21], so it can be considered that this is still a degradation mechanism dominated by HEE. RF overdrive stress generates a strong electric field in the channel of the device, which causes the channel electrons to acquire energy and become hot electrons. These hot electrons will enter the barrier layer or surface of the device, resulting in the decrease of the output current. This mechanism also indicates that for RF overdrive stress, electric field is the main cause of device degradation or failure.

C. LUMINESCENCE CHARACTERISTICS OF THE DEVICES UNDER RF OVERDRIVE STRESS

To further verify the location of defects, EL tests were performed on GaN HEMTs from the same batch. As we known, EL test is an effective means to detect hot electron effects of GaN HEMT [22], [23], [24], [25], [26]. In order to compare the differences of the luminescence characteristics of GaN HEMTs under different RF stresses, EL tests were performed in two RF bias states. The first RF stress state is the saturated input power state, and second is the overdrive input power state, in which the input power is 10dB larger than the saturated input power. The results are shown in Fig. 8.

Fig. 8 (a) and (b) is the EL images in the saturated input power state. As can be seen, the luminescence characteristics of the device are very uniform and each gate of the device is kept at roughly the same brightness. The EL images in the overdrive input power state are shown in Fig. 8 (c) and (d). Compared with EL images in Fig. 8 (a) and (b), the luminescence characteristics of the device become significantly uneven. Lots of bright-spots (shown as pink blobs) appeared in every gate. These bright-spots correspond to the position with more obvious HEE and stronger electric field in the channel. Because hot electrons have high energy and can give rise to photon emission, which appear as discontinuous bright spots on the EL images [27], [28], [29]. Fig. 8(c) and (d) confirm that the hot electron effect is the main mechanism leading to the degradation of devices under RF overdrive stress. It can also be seen the position with the most bright-spots corresponds to the second gate form the top, which is consistent with where it first burned. This also indicates that the device burnout under RF overdrive stress should be related to the electric field.

D. CORRELATION OF DEVICE BURNOUT LIMIT WITH TEMPERATURE

We also discuss the relationship between device burnout and ambient temperature. By continuously increasing the input power at different ambient temperatures until the device burns out, we obtain the results shown in Fig. 9. The input power is increased from 27dBm to 42dBm and every input power state lasts 1 minute. As can be seen from Fig. 9, there is no significant difference in the input power when the device burns out, even if the ambient temperature increases

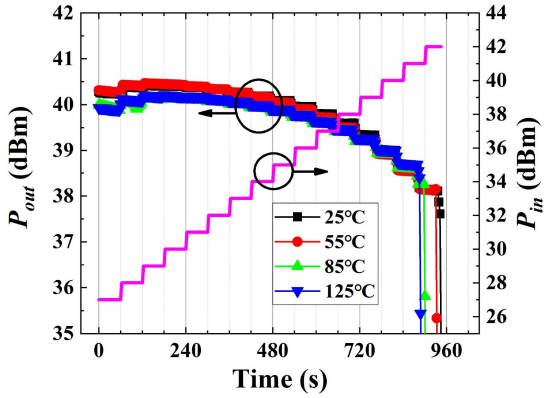

FIGURE 9. RF overdrive burnout limit of devices at different ambient temperatures.

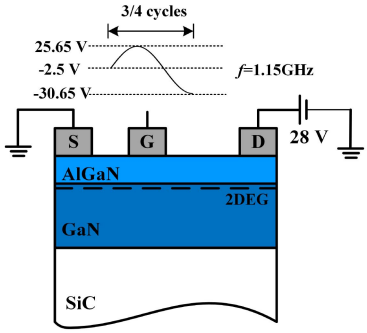

FIGURE 10. The schematic diagram of electrical setup for the TCAD simulation.

by 90 °C. This phenomenon indicates that temperature is not the main factor leading to device burnout.

E. TCAD SIMULATION OF RF OVERDRIVE BURNOUT

In order to further explain that the main cause of device burnout is electric field rather than temperature, we carried out a simulation study on the device by using Silvaco TCAD software. The schematic diagram of electrical setup for the simulation are shown in Fig. 10. The drain voltage is fixed at 28V, the source is grounded and the gate static bias is −2.5V. Then a sinusoidal wave with a frequency of 1.15 GHz and a power of 42 dBm is applied to the gate. According to the input impedance of 50 Ω, the amplitude of the sine wave can be calculated as 28.15V. Considering the static bias of the gate, so the peak of the gate sine wave is 26.65V, and the trough is −30.65V. Obviously, when the trough of the sine wave is applied to the gate, the voltage difference between the gate and drain is the largest, and so is the field strength. Therefore, transient simulation is done at this time to determine the distribution of electric field and temperature inside the device.

Fig. 11 (a) and (b) shows the distribution of lattice temperature and electric field in the device after 3/4 of the gate sine wave period respectively. From the figure, it can be seen that both the highest lattice temperature and the strongest electric field occur between the gate and drain, consistent

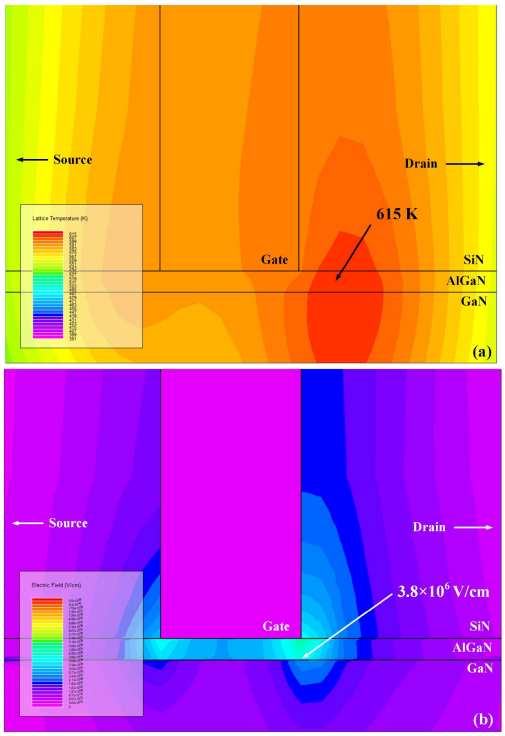

FIGURE 11. The distribution of (a) lattice temperature and (b) electric field in the device after 3/4 of the gate sine wave period.

with the previous analysis. The highest lattice temperature is 615 K, which does not exceed the melting point of any material. While the electric field strength at the AlGaN/GaN interface reaches 3.8 MV/cm, which exceeds the breakdown electric field strength of GaN material (3.3MV/cm). Through the above simulation results, it can be concluded that the burnout under RF overdrive stress is mainly caused by the electric field.

F. MECHANISM ANALYSIS OF BURNOUT BEHAVIORS OF GAN HEMT

A schematic of the physical mechanism of RF overdrive degradation and burnout of AlGaN/GaN HEMTs is shown in Fig. 12. It is well known that GaN devices have a large number of trapping centers at the surface, in the AlGaN barrier layer, at the 2DEG interface, or in the GaN buffer layer [30], [31], [32]. As shown in Fig. 12 (a), when P_{in} is small, the electric field between gate and drain is not so large. It is difficult for the electrons in the channel to obtain enough energy to become hot electrons, and most of them can flow smoothly from the source to the drain, so the luminance of EL image is very uniform, as shown in Fig. 8 (a) and (b). However, when the P_{in} increases, the electric field between the gate drain also increases and a large number of hot electrons are generated. These hot electrons gain enough energy to escape the channel. On the one hand, they can be trapped in the trapping centers as mentioned above [33]. On the other hand, new defects are generated under the gate or in the gate-drain access area, which reduces the output current and make the threshold voltage is drifts

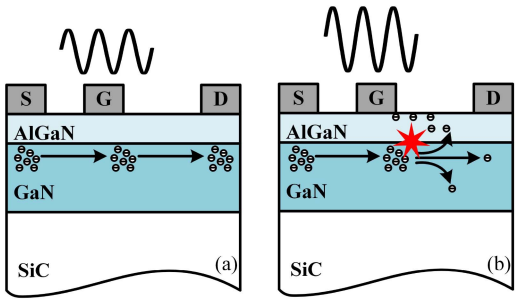

FIGURE 12. Schematic of the physical mechanism of RF overdrive degradation and burnout of AlGaN/GaN HEMTs. (a) Schematic cross section with small P_{in}. (b) Schematic cross section with large P_{in}.

forward, as shown in Fig. 7 (a) and (b) [4], [34], [35]. At last, when P_{in} is further increased, the electric field strength between gate and drain exceeds the breakdown electric field strength of GaN material, resulting in burnout.

According to previous literature reports, there are two mechanisms to explain the burnout of GaN HEMTs. The first is that the forward turn-on of the gate diode exceeds the burnout limit, and the second is the reverse breakdown of the gate-drain junction [36]. In general, the first mechanism occurs when the drain-source voltage is relatively low (<10V), and the second occurs when the drain-source voltage is higher. In the test of this paper, the quiescent drain-source voltage is 28V, which belongs to a high level. Besides, in order to prevent gate voltage drift, a resistor of several thousand ohms is connected in series on the gate to ensure that the gate current will not be too large, which is also a common practice for improving device robustness in applications [37]. It is also reported that the voltage swing of RF overdrive stress leads to the decline of gate breakdown voltage [38], [39]. Therefore, it can be concluded that the burnout failure of this paper is mainly caused by the reverse breakdown of the gate-drain junction. This also explains why the burnout has little to do with ambient temperature.

IV. CONCLUSION

In this paper, we captured the whole process of GaN HEMT burns out under the RF overdrive stress with high speed camera, and located the initial burning spot. Based on long-term stress experiment and EL test, it is confirmed that electric field plays a key role in device burnout. By studying the correlation between the burnout limit and ambient temperature, we found that temperature has little effect on burnout. Through TCAD simulation, it can be shown that the electric field of AlGaN/GaN interface reached 3.8 MV/cm when burnout, which exceeds the breakdown electric field strength of GaN material. Combining with previous literature reports, we believe the mechanism of GaN HEMT burnout is the reverse breakdown of gate-drain junction. In order to restrain this degradation and failure, the Fe- C co-doped buffer layer, the thinner barrier layer and the optimized gate structure can be used [40], [41], [42]. Related analysis methods and mechanism analysis help to improve the survivability of GaN HEMTs under overstress.

REFERENCES

[1] M. Micovic et al., "High frequency GaN HEMTs for RF MMIC applications," in *IEEE Int. Electron Devices Meeting Tech. Dig.*, Dec. 2016, pp. 3.3.1–3.3.4, doi: 10.1109/IEDM.2016.7838337.

[2] U. K. Mishra, L. Shen, T. E. Kazior, and W. Yi-Feng, "GaN-based RF power devices and amplifiers," *Proc. IEEE*, vol. 96, no. 2, pp. 287–305, Feb. 2008, doi: 10.1109/jproc.2007.911060.

[3] C. Andrei, O. Bengtsson, R. Doerner, S. A. Chevtchenko, W. Heinrich, and M. Rudolph, "Dynamic behaviour of a low-noise amplifier GaN MMIC under input power overdrive," in *Proc. Eur. Microw. Conf. (EuMC)*, Dec. 2016, pp. 231–234, doi: 10.1109/EuMC.2015.7345742.

[4] Q. Chen et al., "Degradation behavior and trap analysis based on low-frequency noise of AlGaN/GaN HEMTs subjected to radio frequency overdrive stress," *IEEE Trans. Electron Devices*, vol. 68, no. 1, pp. 66–71, Jan. 2021, doi: 10.1109/ted.2020.3040698.

[5] A. Chini, V. Di Lecce, F. Fantini, G. Meneghesso, and E. Zanoni, "Analysis of GaN HEMT failure mechanisms during DC and large-signal RF operation," *IEEE Trans. Electron Devices*, vol. 59, no. 5, pp. 1385–1392, May 2012, doi: 10.1109/ted.2012.2188636.

[6] H. P. Rao and G. Bosman, "Study of RF reliability of GaN HEMTs using low-frequency noise spectroscopy," *IEEE Trans. Device Mater. Rel.*, vol. 12, no. 1, pp. 31–36, Mar. 2012, doi: 10.1109/tdmr.2011.2173497.

[7] Y. Xie, R. Chen, C. Liu, Y. Chen, and Y. Ren, "Analysis of GaN HEMT degradation under RF overdrive stress," in *Proc. IEEE Workshop Wide Bandgap Power Devices Appl. Asia (WiPDA Asia)*, Aug. 2021, pp. 31–35, doi: 10.1109/WiPDAAsia51810.2021.9656103.

[8] L. Zhou et al., "Investigation on failure mechanisms of GaN HEMT caused by high-power microwave (HPM) pulses," *IEEE Trans. Electromagn. Compat.*, vol. 59, no. 3, pp. 902–909, Jun. 2017, doi: 10.1109/temc.2016.2628046.

[9] L. Zhou, Z.-W. San, L. Lin, and W.-Y. Yin, "Electro-thermal-stress interaction of GaN HEMT breakdown induced by high power microwave pulses," in *Proc. Asia–Pacific Int. Symp. Electromagn. Compat. (APEMC)*, May 2016, pp. 642–644, doi: 10.1109/APEMC.2016.7522823.

[10] C. Liu et al., "Effect of atmosphere on electrical characteristics of AlGaN/GaN HEMTs under hot-electron stress," *IEEE Trans. Electron Devices*, vol. 68, no. 3, pp. 1000–1005, Mar. 2021, doi: 10.1109/ted.2021.3049764.

[11] S. Xiong and Z. Du, "Burnout effects of microwave pulses on the AlGaN/GaN HEMT in an LNA," in *Proc. IEEE 5th Int. Symp. Electromagn. Compat. (EMC)*, Oct. 2017, pp. 1–5, doi: 10.1109/EMC-B.2017.8260405.

[12] L. Liu and Z. Du, "Influence of microwave pulse power on the burnout effect of the AlGaN/GaN HEMT in a LNA," in *Proc. IEEE 6th Int. Symp. Electromagn. Compat. (ISEMC)*, Nov. 2019, pp. 1–5, doi: 10.1109/ISEMC48616.2019.8986032.

[13] S. Liu et al., "Simulation research on single event burnout performances of p-GaN gate HEMTs with 2DEG $Al_xGa_{1-x}N$ channel," *IEEE Trans. Electron Devices*, vol. 69, no. 3, pp. 973–980, Mar. 2022, doi: 10.1109/ted.2022.3141985.

[14] W. Junbo, Z. Yan, Y. Minge, D. Bingjun, and Y. Zhimao, "Observation of arc discharging process of nanocomposite Ag–SnO2 and La-doped Ag–SnO2 contact with a high-speed camera," *Mater. Sci. Eng. B*, vol. 131, nos. 1–3, pp. 230–234, Jul. 2006, doi: 10.1016/j.mseb.2006.04.042.

[15] L. Zhang, E. Binner, Y. Qiao, and C. Z. Li, "High-speed camera observation of coal combustion in air and O_2/CO_2 mixtures and measurement of burning coal particle velocity," *Energy Fuels*, vol. 24, no. 1, pp. 29–37, Sep. 2009, doi: 10.1021/ef900463r.

[16] R. J. Trew and U. K. Mishra, "Gate breakdown in MESFETs and HEMTs," *IEEE Electron Device Lett.*, vol. 12, no. 10, pp. 524–526, Oct. 1991, doi: 10.1109/55.119177.

[17] G. Deva et al., "Investigation of AlGaN/GaN HEMT breakdown analysis with source field plate length for high power applications," in *Proc. 5th Int. Conf. Devices, Circuits Syst. (ICDCS)*, Mar. 2020, pp. 244–246, doi: 10.1109/ICDCS48716.2020.243589.

[18] H. Yu et al., "Improvement of breakdown characteristics in AlGaN/GaN/AlxGa1-xN HEMT based on a grading AlxGa1-xN buffer layer," *Physica Status Solidi A*, vol. 207, no. 11, pp. 2593–2596, Aug. 2010, doi: 10.1002/pssa.201026270.

[19] Z. Chang et al., "On the degradation kinetics and mechanism of AlGaN/GaN HEMTs under high temperature operation(HTO) stress," in *Proc. IEEE Int. Conf. Electron Devices Solid-State Circuits*, Mar. 2015, pp. 1–2, doi: 10.1109/EDSSC.2014.7061278.
[20] A. Benvegnù et al., "Characterization of defects in AlGaN/GaN HEMTs based on nonlinear microwave current transient spectroscopy," *IEEE Trans. Electron Devices*, vol. 64, no. 5, pp. 2135–2141, May 2017, doi: 10.1109/TED.2017.2682112.
[21] B. M. Paine, S. R. Polmanter, V. T. Ng, N. T. Kubota, and C. R. Ignacio, "Lifetesting GaN HEMTs with multiple degradation mechanisms," *IEEE Trans. Device Mater. Rel.*, vol. 15, no. 4, pp. 486–494, Dec. 2015, doi: 10.1109/TDMR.2015.2474359.
[22] Y. Puzyrev et al., "Gate bias dependence of defect-mediated hot-carrier degradation in GaN HEMTs," *IEEE Trans. Electron Devices*, vol. 61, no. 5, pp. 1316–1320, May 2014, doi: 10.1109/ted.2014.2309278.
[23] T. Brazzini et al., "Electroluminescence of hot electrons in AlGaN/GaN high-electron-mobility transistors under radio frequency operation," *Appl. Phys. Lett.*, vol. 106, no. 21, May 2015, Art. no. 213502, doi: 10.1063/1.4921848.
[24] Y. Wang, X. Hong, C. Zeng, P. Lai, and Y. Huang, "Reliability evaluation and failure analysis of AlGaN/GaN high electron mobility transistor by photo emission microscope," in *Proc. 20th IEEE Int. Symp. Phys. Failure Anal. Integr. Circuits (IPFA)*, Jul. 2013, pp. 259–262, doi: 10.1109/IPFA.2013.6599164.
[25] T. Brazzini et al., "Hot-electron electroluminescence under RF operation in GaN-HEMTs: A comparison among operational classes," *IEEE Trans. Electron Devices*, vol. 64, no. 5, pp. 2155–2160, May 2017, doi: 10.1109/ted.2017.2686782.
[26] M. Meneghini, A. Stocco, R. Silvestri, G. Meneghesso, and E. Zanoni, "Degradation of AlGaN/GaN high electron mobility transistors related to hot electrons," *Appl. Phys. Lett.*, vol. 100, no. 23, Jun. 2012, Art. no. 233508, doi: 10.1063/1.4723848.
[27] M. Meneghini et al., "Investigation of trapping and hot-electron effects in GaN HEMTs by means of a combined electrooptical method," *IEEE Trans. Electron Devices*, vol. 58, no. 9, pp. 2996–3003, Sep. 2011, doi: 10.1109/ted.2011.2160547.
[28] M. Meneghini, G. Meneghesso, and E. Zanoni, "Analysis of the reliability of AlGaN/GaN HEMTs submitted to on-state stress based on electroluminescence investigation," *IEEE Trans. Device Mater. Rel.*, vol. 13, no. 2, pp. 357–361, Jun. 2013, doi: 10.1109/tdmr.2013.2257783.
[29] G. Meneghesso et al., "Reliability of GaN high-electron-mobility transistors: State of the art and perspectives," *IEEE Trans. Device Mater. Rel.*, vol. 8, no. 2, pp. 332–343, Jun. 2008, doi: 10.1109/tdmr.2008.923743.
[30] S. C. Binari, P. B. Klein, and T. E. Kazior, "Trapping effects in wide-bandgap microwave FETs," in *IEEE MTT-S Int. Microw. Symp. Dig.*, Jun. 2002, pp. 1823–1826, doi: 10.1109/MWSYM.2002.1012217.
[31] J. M. Tirado, J. L. Sanchez-Rojas, and J. I. Izpura, "Trapping effects in the transient response of AlGaN/GaN HEMT devices," *IEEE Trans. Electron Devices*, vol. 54, no. 3, pp. 410–417, Mar. 2007, doi: 10.1109/ted.2006.890592.
[32] R. Vetury, N. Q. Zhang, S. Keller, and U. K. Mishra, "The impact of surface states on the DC and RF characteristics of AlGaN/GaN HFETs," *IEEE Trans. Electron Devices*, vol. 48, no. 3, pp. 560–566, Mar. 2001, doi: 10.1109/16.906451.
[33] E. Zanoni et al., "Reliability of gallium nitride microwave transistors," in *Proc. 21st Int. Conf. Microw. Radar Wireless Commun. (MIKON)*, May 2016, pp. 1–6, doi: 10.1109/MIKON.2016.7492013.
[34] M. Caesar et al., "Generation of traps in AlGaN/GaN HEMTs during RF-and DC-stress test," in *Proc. IEEE Int. Rel. Phys. Symp. (IRPS)*, Apr. 2012, pp. CD.6.1–CD.6.5, doi: 10.1109/IRPS.2012.6241883.
[35] N. Moultif et al., "Reliability assessment Of AlGaN/GaN HEMTs on the SiC substrate under the RF stress," *IEEE Trans. Power Electron.*, vol. 36, no. 7, pp. 7442–7450, Jul. 2021, doi: 10.1109/tpel.2020.3042133.
[36] Y. Chen et al., "Survivability of AlGaN/GaN HEMT," in *IEEE MTT-S Int. Microw. Symp. Tech. Dig.*, Jul. 2007, pp. 307–310, doi: 10.1109/MWSYM.2007.380413.
[37] M. Rudolph et al., "Analysis of the survivability of GaN low-noise amplifiers," *IEEE Trans. Microw. Theory Techn.*, vol. 55, no. 1, pp. 37–43, Jan. 2007, doi: 10.1109/tmtt.2006.886907.
[38] H. Kim et al., "Reliability evaluation of high power AlGaN/GaN HEMTs on SiC substrate," *Physica Status Solidi A*, vol. 188, no. 1, pp. 203–206, Nov. 2001, doi: 10.1002/1521-396X(200111)188:1<203::AID-PSSA203>3.0.CO;2-C.
[39] H. Hasegawa, K. Katsukawa,T. Itoh, T. Noguchi, and Y. Kaneko, "High reliability power GaAs MESFET under RF overdrive condition," in *IEEE MTT-S Int. Microw. Symp. Dig.*, Jun. 1993, pp. 289–292, doi: 10.1109/MWSYM.1993.276821.
[40] D. Bisi et al., "Hot-electron degradation of AlGaN/GaN high-electron mobility transistors during RF operation: Correlation with GaN buffer design," *IEEE Electron Device Lett.*, vol. 36, no. 10, pp. 1011–1014, Oct. 2015, doi: 10.1109/led.2015.2474116.
[41] C. Lee et al., "Effects of AlGaN/GaN HEMT structure on RF reliability," *Electron. Lett.*, vol. 41, no. 3, pp. 155–157, Mar. 2005, doi: 10.1049/el:20057802.
[42] R. Vetury et al., "Performance and RF reliability of GaN-on-SiC HEMT's using dual-gate architectures," in *IEEE MTT-S Int. Microw. Symp. Dig.*, Jul. 2006, pp. 714–717, doi: 10.1109/MWSYM.2006.249733.